

Reduction of O₂ to Superoxide Anion (O₂^{•-}) in Water by Heteropolytungstate Cluster-Anions

Yurii V. Geletii,[†] Craig L. Hill,[†] Rajai H. Atalla,[‡] and Ira A. Weinstock^{*,§,#}

Contribution from the Department of Chemistry, Emory University, Atlanta, Georgia 30322, Chemistry and Pulping Research Work Unit, USDA Forest Products Laboratory, Madison, Wisconsin 50726, and Department of Chemistry, City College of The City University of New York, New York, New York 10031

Received June 28, 2006; E-mail: iraw@bgu.ac.il

Abstract: Fundamental information concerning the mechanism of electron transfer from reduced heteropolytungstates (POM_{red}) to O₂, and the effect of donor-ion charge on reduction of O₂ to superoxide anion (O₂^{•-}), is obtained using an isostructural series of 1e⁻-reduced donors: α -Xⁿ⁺W₁₂O₄₀⁽⁹⁻ⁿ⁾⁻, Xⁿ⁺ = Al³⁺, Si⁴⁺, P⁵⁺. For all three, a single rate expression is observed: $-d[\text{POM}_{\text{red}}]/dt = 2k_{12}[\text{POM}_{\text{red}}][\text{O}_2]$, where k_{12} is for the rate-limiting electron transfer from POM_{red} to O₂. At pH 2 (175 mM ionic strength), k_{12} increases from 1.4 ± 0.2 to 8.5 ± 1 to $24 \pm 2 \text{ M}^{-1}\text{s}^{-1}$ as Xⁿ⁺ is varied from P⁵⁺ (3_{red}) to Si⁴⁺ (2_{red}) to Al³⁺ (1_{red}). Variable-pH data (for 1_{red}) and solvent-kinetic isotope (KIE = $k_{\text{H}}/k_{\text{D}}$) data (all three ions) indicate that protonated superoxide (HO₂[•]) is formed in two steps—electron transfer, followed by proton transfer (ET–PT mechanism)—rather than via simultaneous proton-coupled electron transfer (PCET). Support for an outersphere mechanism is provided by agreement between experimental k_{12} values and those calculated using the Marcus cross relation. Further evidence is provided by the small variation in k_{12} observed when Xⁿ⁺ is changed from P⁵⁺ to Si⁴⁺ to Al³⁺, and the driving force for formation of O₂^{•-} (aq), which increases as cluster-anion charge becomes more negative, increases by nearly +0.4 V (a decrease of > 9 kcal mol⁻¹ in ΔG°). The weak dependence of k_{12} on POM reduction potentials reflects the outersphere ET–PT mechanism: as the anions become more negatively charged, the “successor-complex” ion pairs are subject to larger anion–anion repulsions, in the order [(3_{ox}³⁻)(O₂^{•-})]⁴⁻ < [(2_{ox}⁴⁻)(O₂^{•-})]⁵⁻ < [(1_{ox}⁵⁻)(O₂^{•-})]⁶⁻. This reveals an inherent limitation to the use of heteropolytungstate charge and reduction potential to control rates of electron transfer to O₂ under turnover conditions in catalysis.

Introduction

The reduction of O₂ is fundamental to processes ranging from the carefully orchestrated reactions in living cells to the radical-chain reactions that, because they are so difficult to control, prevent the more rapid design and implementation of O₂-based technologies.¹ Among the many types of molecular complexes used to control the reactions of O₂, polymeric metal-oxide cluster-anion (polyoxometalates, or POMs), are consistently featured in reports that document notable advances in this area.^{2–8} In addition, because many POMs possess reversible

redox chemistries and are well defined and stable in solution, they are deployed as physicochemical probes of electron-transfer processes. In the present study, a representative series of 1e⁻-reduced Keggin heteropolytungstates are used to establish the mechanism of electron transfer from these cluster anions to O₂, and simultaneously, as well-defined probes to quantify the effects of donor-ion charge on the reduction of O₂ to O₂^{•-}.

As noted, POMs are used to catalyze a wide and rapidly expanding range of selective oxidation and reduction processes.⁹ These involve the use of POMs in heterogeneous⁷ and electrochemical catalysis^{8,10} (including as components of modified electrodes),^{11,12} and as homogeneous catalysts in both thermal¹⁵ and photochemical processes.¹³ In catalysis, turnover often involves the transfer of electrons from reduced cluster anions to substrates or other reactants.¹⁴ Not surprisingly, the rational

[†] Emory University.

[‡] USDA Forest Products Laboratory.

[§] City College of The City University of New York.

[#] Current address: Department of Chemistry, Ben Gurion University, Beer Sheva, 84105, Israel.

- Hill, C. L.; Weinstock, I. A. *Nature* **1997**, *388*, 332–333.
- Renneke, R. F.; Hill, C. L. *J. Am. Chem. Soc.* **1986**, *108*, 3528–9.
- Neumann, R.; Dahan, M. *Nature* **1997**, *388*, 353–355.
- Weiner, H.; Finke, R. G. *J. Am. Chem. Soc.* **1999**, *121*, 9831–9842.
- Weinstock, I. A.; Barbuzzi, E. M. G.; Wemple, M. W.; Cowan, J. J.; Reiner, R. S.; Sonnen, D. M.; Heintz, R. A.; Bond, J. S.; Hill, C. L. *Nature* **2001**, *414*, 191–195.
- Kamata, K.; Yonehara, K.; Sumida, Y.; Yamaguchi, K.; Hikichi, S.; Mizuno, N. *Science* **2003**, *300*, 964–966.
- Bar-Nahum, I.; Khenkin, A. M.; Neumann, R. *J. Am. Chem. Soc.* **2004**, *126*, 10236–10237.
- Kim, W. B.; Voitl, T.; Rodriguez-Rivera, G. J.; Dumesic, J. A. *Science* **2004**, *305*, 1280–1283.

- Hill, C. L. In *Comprehensive Coordination Chemistry II: From Biology to Nanotechnology*; Wedd, A. G., Ed.; Elsevier: Oxford, 2004; Vol. 4, p 679–759.
- Toth, J. E.; Anson, F. C. *J. Am. Chem. Soc.* **1989**, *111*, 2444–2451.
- Teague, C. M.; Li, X.; Biggin, M. E.; Lee, L.; Kim, J.; Gewirth, A. A. *J. Phys. Chem. B* **2004**, *108*, 1974–1985.
- Zhang, J.; Goh, J.-K.; Tan, W.-T.; Bond, A. M. *Inorg. Chem.* **2006**, *45*, 3732–3740.
- Hill, C. L.; Prosser-McCartha, C. M. In *Photosensitization and Photocatalysis Using Inorganic and Organometallic Compounds*; Kalyanasundaram, K., Grätzel, M., Eds.; Kluwer Academic Publishers: Dordrecht, The Netherlands, 1993; Vol. 14, p 307–330.

design of new POM catalysts requires a fundamental understanding of the underlying electron-transfer processes.^{15,16}

As a class, POMs are inherently stable to strongly oxidizing conditions that would rapidly oxidize and degrade the organic ligands of most metallo-organic complexes.^{5,17–19} This, coupled with the ease with which the composition, structure and physical properties of POMs can be readily and rationally altered,²⁰ has led to a large and rapidly growing list of reactions wherein these cluster anions are deployed as catalysts for selective oxidations by O₂.^{3,9,21} For this, water and O₂—while not always practical because of substrate insolubility—are the most economically and environmentally desirable solvent and oxidant.^{22,23} Whether in water or organic solvents, however, the reaction between reduced POMs and O₂ is of central importance.

Reduced molybdovanadophosphates, notably, reduced (V(IV)-containing) forms of the fully oxidized cluster, PV₂Mo₁₀O₄₀⁵⁻ (historically, the most widely reported POM cluster for use in catalytic oxidation processes) are believed to react with O₂ via an innersphere pathway.²⁴ While this has yet to be fully established,^{25–27} an innersphere mechanism is consistent with the relatively labile nature of Mo–O bonds,^{24,26,28,29} and with the tendency of vanadyl ions, [V^{IV}=O]²⁺, to dissociate from reduced forms of PV₂Mo₁₀O₄₀⁵⁻ in solution.²⁷

While reduced heteropolytungstates are more likely to react with O₂ via an outersphere mechanism,¹⁴ the few studies that address this question lead to contradictory conclusions. In 1985, Darwent³⁰ reported that reactions between Keggin heteropolytungstates and O₂, observed during the photochemical oxidation of isopropanol (10% in water), were first order in both [O₂] and [H⁺]. Despite the complexity inherent in this system, the [H⁺] dependence was attributed to protonation of incipient superoxide radical anion (O₂^{•-}) in the transition-state, during rate-limiting electron transfer to O₂. A linear plot of ln *k* versus Δ*G*^o/*RT*, for reactions of several reduced Keggin anions at pH 1, gave a slope of 0.52, the value expected for an outersphere mechanism. At pH 1, however, the more negatively charged donor anions studied are protonated.^{31–37} This has substantial energetic and mechanistic consequences.¹⁵ Because these were

not addressed, the meaning of the free-energy relationship remains uncertain.

This uncertainty left room for the subsequent publication (1992) of data—obtained using some of the same Keggin anions—that were interpreted as evidence in support of an innersphere mechanism. In that study,³⁸ Papaconstantinou observed a complex [H⁺] dependence for reactions of the one-electron reduced anions, SiW₁₂O₄₀⁵⁻ and P₂W₁₈O₆₂⁷⁻ at pH values of between 1.5 and 3. This was interpreted as evidence of an innersphere mechanism involving the formation of an intermediate that contained a W(V)–O₂ bond. The complex H⁺ dependence was attributed to pH-dependent protonation of the coordinated superoxide anion (W(VI)–O₂⁻).

More recently, Duncan and Hill reported³⁹ that upon complete reduction of labeled O₂ to H₂O by reduced heteropolytungstates, and by PMo₁₂O₄₀⁴⁻, the label was initially found only in H₂O and not in the structure of the (then) oxidized POMs. While not definitive, this product study was consistent with an outersphere mechanism. However, an innersphere process could not be ruled out: an identical result was obtained using the reduced form of PV₂Mo₁₀O₄₀⁵⁻, which, as noted above, is believed to react with O₂ via an innersphere mechanism.

We now provide a definitive study of electron transfer from reduced Keggin heteropolytungstates to O₂. This is accomplished using an isostructural series of cluster anions, α-Keggin-X^{*n*+}W₁₂O₄₀^{(9-*n*)-}, whose charges vary from 6⁻ to 5⁻ to 4⁻ as the central heteroatom, X^{*n*+}, is changed from Al³⁺ to Si⁴⁺ to P⁵⁺. As a result of these efforts, the mechanism by which this large and representative subclass of POMs reacts with O₂ is firmly established. Issues addressed include assessment of the role of H⁺ using α-Al³⁺W₁₂O₄₀⁶⁻ (X^{*n*+} = Al³⁺)^{40–42} which, unlike the other anions in the series, is stable between pH values of 1.8 and 7.5.^{16,43,44} Conclusions include the role of Keggin-charge on reaction rates, attendant implications for the

(14) Weinstock, I. A. *Chem. Rev.* **1998**, *98*, 113–170.

(15) Grigoriev, V. A.; Cheng, D.; Hill, C. L.; Weinstock, I. A. *J. Am. Chem. Soc.* **2001**, *123*, 5292–5307.

(16) Geletii, Y. V.; Hill, C. L.; Bailey, A. J.; Hardcastle, K. I.; Atalla, R. H.; Weinstock, I. A. *Inorg. Chem.* **2005**, *44*, 8955–8966.

(17) Katsoulis, D. E.; Pope, M. T. *J. Am. Chem. Soc.* **1984**, *106*, 2737–2738.

(18) Hill, C. L.; Brown, R. B., Jr. *J. Am. Chem. Soc.* **1986**, *108*, 536–538.

(19) Mansuy, D.; Bartoli, J.-F.; Battioni, P.; Lyon, D. K.; Finke, R. G. *J. Am. Chem. Soc.* **1991**, *113*, 7222–7226.

(20) Pope, M. T. In *Comprehensive Coordination Chemistry II: From Biology to Nanotechnology*; Wedd, A. G., Ed.; Elsevier Ltd.: Oxford, 2004; Vol. 4, p 635–678.

(21) Neumann, R. *Prog. Inorg. Chem.* **1998**, *47*, 317–370.

(22) Hill, C. L. *Nature* **1999**, *401*, 436–437.

(23) Botar, B.; Geletii, Y. V.; Kögerler, P.; Musaev, D. G.; Morokuma, K.; Weinstock, I. A.; Hill, C. L. *J. Am. Chem. Soc.* **2006**, *128*, 11268–11277.

(24) Neumann, R.; Levin, M. *J. Am. Chem. Soc.* **1992**, *114*, 7278–7286.

(25) Efforts to clarify the mechanism of this reaction are complicated by the presence in solutions of H₅PV₂Mo₁₀O₄₀ of (1) positional isomers (5 relative positions of the two V ions), (2) structural isomers (α and β), (3) small equilibrium concentrations of the mono- and trivanadium anions, H₄PVMo₁₁O₄₀ and H₆PV₃Mo₉O₄₀, and (4) equilibria between bound and dissociated vanadyl, V^{IV}=O²⁺, ions (see refs 26 and 27).

(26) Pettersson, L.; Andersson, I.; Selling, A.; Grate, G. H. *Inorg. Chem.* **1994**, *33*, 982–993.

(27) Kozhevnikov, I. V. *Chem. Rev.* **1998**, *98*, 171–198.

(28) An example of this is Mars-van Krevelen-type oxo-transfer chemistry documented by Neumann, Khenkin, and co-workers in ref 29.

(29) Khenkin, A. M.; Weiner, L.; Wang, Y.; Neumann, R. *J. Am. Chem. Soc.* **2001**, *123*, 8531–8542.

(30) Akid, R.; Darwent, J. R. *J. Chem. Soc., Dalton Trans.* **1985**, 395–399.

- (31) In the reported free-energy relationship, the Gibbs free energy (Δ*G*^o) was calculated using the reduction potential, *E*_{1/2}, of the O₂/HO₂[•] couple, consistent with the formation of HO₂[•] (protonation by solvent, see ref 32) in the transition state. Indeed, the Marcus cross relation has been applied successfully to proton-coupled electron transfer (PCET) reactions (refs 33–34.). Here, however, Fe^{III}W₁₂O₄₀⁷⁻ (the most reactive of the four anions studied) was not only reduced by two electrons but, at pH 1, is also partially-protonated (i.e., present as the conjugate-acid), while PW₁₂O₄₀⁴⁻ (included in the same plot) is not. In such cases it is necessary to differentiate simultaneous electron and proton transfer from situations in which “the pH dependence arises from the distribution between acid and base forms and not from variations in the driving force” (quoted from ref 35). The reaction could also be catalyzed by protonation of O₂^{•-} by protons associated with reduced POMs. This would be analogous to reactions described in refs 36–37. While intriguing, the data reported by Darwent highlight the need, when studying reactions of POM salts, to fully define the nature and concentrations of dynamic ion pairs present in solution.
- (32) Nets, P.; Huie, R. E.; Maruthamuth, P.; Steenken, S. *J. Phys. Chem.* **1989**, *93*, 7654–7659.
- (33) Roth, J. P.; Yoder, J. C.; Won, T.-J.; Mayer, J. M. *Science* **2001**, *294*, 2524–2526.
- (34) Mayer, J. M. *Annu. Rev. Phys. Chem.* **2004**, *55*, 363–390.
- (35) Lebeau, E. L.; Binstead, R. A.; Meyer, T. J. *J. Am. Chem. Soc.* **2001**, *123*, 10535–10544.
- (36) Bernhard, P.; Sargeson, A. M.; Anson, F. C. *Inorg. Chem.* **1988**, *27*, 2154–2760.
- (37) Bacac, A.; Espenson, J. H.; Creaser, I. I.; Sargeson, A. M. *J. Am. Chem. Soc.* **1983**, *105*, 7624–7628.
- (38) Hiskia, A.; Papaconstantinou, E. *Inorg. Chem.* **1992**, *31*, 163–167.
- (39) Duncan, D. C.; Hill, C. L. *J. Am. Chem. Soc.* **1997**, *119*, 243–244.
- (40) Cowan, J. J.; Hill, C. L.; Reiner, R. S.; Weinstock, I. A. In *Inorganic Syntheses*; Coucouvanis, D., Ed.; John Wiley & Sons, Inc.: New York, 2002; Vol. 33, p 18–26.
- (41) Weinstock, I. A.; Cowan, J. J.; Barbuzzi, E. M. G.; Zeng, H.; Hill, C. L. *J. Am. Chem. Soc.* **1999**, *121*, 4608–4617.
- (42) Cowan, J. J.; Bailey, A. J.; Heintz, R. A.; Do, B. T.; Hardcastle, K. I.; Hill, C. L.; Weinstock, I. A. *Inorg. Chem.* **2001**, *40*, 6666–6675.
- (43) Geletii, Y. V.; Weinstock, I. A. *J. Mol. Catal. A: Chem.* **2006**, *251* 255–262.

rational design of heteropolytungstate catalysts for selective oxidations by O₂, and quantitative information about the effect of the anion–anion repulsion that accompanies the formation of successor-complex ion pairs, [(α -Xⁿ⁺W₁₂O₄₀⁽⁸⁻ⁿ⁾⁻)(O₂^{•-})].

Materials and Methods

Synthesis and Characterization. Fully oxidized α -Keggin ions (POM_{ox}; all W atoms in their highest, +6, d⁰, oxidation states), α -Na₅-Al^{III}W₁₂O₄₀, (**1**_{ox}),^{40–42} and α -Na₄Si^{IV}W₁₂O₄₀, (**2**_{ox}),⁴⁵ were prepared using published methods; α -Na₃PW₁₂O₄₀, (**3**_{ox}), was purchased from Sigma-Aldrich, Inc. One-electron reduced forms of the above anions, POM_{red}, that is, α -Al^{III}W₁₂O₄₀⁶⁻, (**1**_{red}), α -Si^{IV}W₁₂O₄₀⁵⁻, (**2**_{red}), and α -P^VW₁₂O₄₀⁴⁻, (**3**_{red}), were prepared in water by constant-potential electrolysis, quantified, as previously described for **1** and **3**,^{16,43} and stored under argon. All other materials were purchased from commercial sources.

Aqueous Solutions. Solutions were prepared using water from a Barnstead Nanopure water-purification system and added salts, buffers, and chelating agents were of the highest purity available. Specific ionic strengths were obtained by adding NaCl, and reported ionic-strength values of POM-containing solutions include contributions from the POM salts themselves. pD values of solutions in D₂O were calculated using pD = pH_{el} + 0.4, where pH_{el} was read from a standard pH electrode immersed in the D₂O solution.^{46,47} Small deviations from target pH (pD) values, caused by additions of NaCl or POM salts to pH-adjusted buffered solutions, were compensated for by additions of small quantities of HCl or NaOH.

Instrumentation. UV–vis spectra were acquired using Hewlett-Packard 8452A or StellarNet Inc. EPP2000 spectrophotometers equipped with diode-array detectors and an immersible fiber-optic probe. The Hewlett-Packard 8452A instrument was equipped with a magnetic stirrer and temperature controller (HP 89090A). Electrochemical data were obtained at room temperature using a BAS CV-50W electrochemical analyzer equipped with a glassy-carbon working electrode, a Pt-wire auxiliary electrode, and a Ag/AgCl (3 M NaCl) BAS reference electrode. All reduction potentials are reported relative to the normal hydrogen electrode (NHE). pH measurements were made using an Orion 250A pH meter. Reaction rates were measured using an SF-61 stopped-flow instrument (Hi-Tech Scientific, U.K.). Al-27 NMR spectra^{16,41} were acquired on a GE QE300 MHz spectrometer at 78.216 Mhz, using a pulse width of 15 μ s and a sweep width of 12500 Hz. Reported chemical-shift values are referenced to 0.1 M AlCl₃ in 1.0 M aqueous HCl ([Al(H₂O)₆]³⁺, δ = 0 ppm) placed in the inner compartment of coaxial NMR tubes. The reference solutions were also used as external standards for integration of ²⁷Al NMR signals. Internal lock signals were tuned using D₂O. Spectral data were processed using the NMR software package, NUTS (1-D version, Acorn NMR Inc., Fremont, CA).

Electrochemistry. Cyclic voltammograms (CVs), bulk electrolysis, and methods for obtaining accurate extinction coefficients of one-electron reduced α -Keggin anions were as previously described.¹⁶ Key aspects are summarized here. All electrochemical data was obtained at room temperature (24 \pm 2 °C). CVs were obtained using 1 to 6 mM POM concentrations in buffered solutions, ionic strengths of from 0.05 to 1.20 M, adjusted by the addition of NaCl, the Ag/AgCl (3 M NaCl) BAS reference electrode, and scan rates of from 20 to 400 mV s⁻¹. The BAS reference electrode was calibrated¹⁶ using the [Fe(CN)₆]³⁻/[Fe(CN)₆]⁴⁻ couple, and the E_{1/2} values reported below are referenced to the NHE by subtraction of 250 mV from BAS electrode values. Aqueous solutions of one-electron reduced α -Keggin anions were

prepared by bulk electrolysis under Ar using a reticulated vitreous-carbon working electrode. Extinction coefficients used in the present work (in M⁻¹ cm⁻¹) are $\epsilon_{700} = (1.56 \pm 0.1) \times 10^3$ and $(1.48 \pm 0.1) \times 10^3$ for **3**_{red} and **2**_{red}, respectively, both at pH 2.1 in sodium sulfate buffer, and $(1.8 \pm 0.1) \times 10^3$ for **1**_{red} at both pH 2.1 in sodium sulfate buffer and pH 7.2 in sodium phosphate buffer.

O₂ Concentrations. The concentration of dioxygen, [O₂], in pure water at 25 °C and 1 atm total pressure (760 Torr; P(O₂) + P(H₂O)) is 1.24 mM. The solubility of O₂ is smaller in aqueous electrolyte solutions than in pure water and depends slightly on the nature of the electrolyte. In this work, total salt concentrations typically did not exceed 200 mM—in most reactions with O₂, a “standard” ionic strength of 175 mM was maintained. Depending upon the electrolyte used, salt concentrations in this range usually result in 6 to 10% decreases in O₂ solubility.⁴⁸ Therefore, O₂ concentrations in our electrolyte solutions, prepared by saturation with O₂ at room temperature (24 \pm 2 °C) and ambient pressure, were assigned a common value of 1.15 mM, 8% smaller than that in pure water. This value was then used for evaluation of kinetic data obtained using a stopped-flow apparatus at 25 °C in thermostated cells. (Changes in O₂ concentrations because of variation in ambient temperatures (24 \pm 2 °C) were smaller than the 5–8% uncertainties in measured rate constants.) In most stopped-flow kinetic measurements, O₂-free POM_{red} solutions were rapidly mixed in 1:1 v/v ratios with aqueous electrolyte solutions saturated using specific O₂/Ar mixtures, or with ambient air. This procedure resulted in 50% dilution of the [O₂]-containing component (i.e., 50% dilution of the contents of one of the two syringes in the stopped-flow apparatus). The largest [O₂] thus obtained was 0.575 mM. In several experiments, the range of experimentally obtainable initial-[O₂] values was increased by using a variable-ratio drive—a standard accessory in stopped-flow instruments—to increase the relative volume of the O₂-saturated solution.

Reaction Stoichiometry. In reactions of **2**_{red} or **3**_{red} with O₂ at acidic pH values, 2 equiv are consumed per 1 equiv of O₂.³⁸ Moreover, reported kinetic measurements show that reactions of reduced heteropolytungstates with H₂O₂ are at least an order of magnitude slower than reactions with O₂.¹⁴ To confirm this stoichiometry for reactions of **1**_{red}, solutions at pH 7.2 (NaH₂PO₄/Na₂HPO₄ buffer) and at pH 2 (NaHSO₄/Na₂SO₄ buffer) were saturated with O₂ and rapidly mixed with solutions of **1**_{red} in a stopped-flow apparatus. The initial absorbance of the reaction mixtures at 700 nm ($\epsilon = (1.8 \pm 0.1) \times 10^3$ M⁻¹ cm⁻¹) provided precise values for the initial concentrations of **1**_{red}. After mixing, the solutions were collected in a flask that had been filled with pure O₂. Once all the blue color associated with **1**_{red} had been discharged, an 0.5 mL aliquot of the now colorless solution was transferred to a UV–vis cell that contained 2 mL of a 5 mM solution of H₅TiPW₁₁O₄₀⁴⁹ in 0.8 M H₂SO₄. Under these conditions, 5 min are sufficient for the reaction with H₂O₂ to give the yellow (TiO₂)PW₁₁O₃₉⁵⁻ peroxy-complex^{49,50} ($\lambda_{\max} = 392$ nm) in quantitative yield. In a separate control experiment, identical conditions were used to determine the extinction coefficient of authentic (TiO₂)PW₁₁O₃₉⁵⁻: $\epsilon_{392} = (1.7 \pm 0.1) \times 10^3$ M⁻¹ cm⁻¹, which is in good agreement with the published value of 1.6×10^3 M⁻¹ cm⁻¹.⁴⁹ Concentrations of H₂O₂ in aqueous stock solutions were determined by UV–vis, using $\epsilon_{254} = (19.6 \pm 0.3)$ M⁻¹ cm⁻¹.⁵¹ Data provided in the Results section show that 2 equiv of **1**_{red} react with O₂ to give 1 equiv of H₂O₂.

Oxidation of **1_{red} by H₂O₂.** The stoichiometry of the reaction between **1**_{red} and H₂O₂ was determined by mixing H₂O₂ (0.1 to 0.5 mM) with **1**_{red} (0.3 to 1.1 mM) in a stopped-flow instrument under Ar, with **1**_{red} always in excess over H₂O₂. The amount of **1**_{red} consumed

- (44) Studies at lower pH values that fully take into account the protonation states of all reduced and fully oxidized Keggin anions involved are in progress.
 (45) Pope, M. T.; Varga, G. M., Jr. *Inorg. Chem.* **1966**, *5*, 1249–1254.
 (46) Westcott, C. C. *pH Measurements*; Academic Press: New York, 1978.
 (47) Kim, G.-S.; Zeng, H.; Neiwert, W. A.; Cowan, J. J.; VanDerveer, D.; Hill, C. L.; Weinstock, I. A. *Inorg. Chem.* **2003**, *42*, 5537–5544.

- (48) Clever, H. L.; Young, C. L.; Battino, R.; Derrick, M. E.; Katovic, V.; Pogrebnya, V. L.; Usov, A. P.; Baranov, A. V. *Solubility Data Ser.* **1981**, *7*, 56–189.
 (49) Maksimov, G. M.; Kuznetsova, L. I.; Matveev, K. I.; Maksimovskaya, R. I. *Koord. Khim.* **1985**, *11*, 1353–1357.
 (50) Detusheva, L. G.; Fedotov, M. A.; Kuznetsova, L. I.; Vlasov, A. A.; Likhobolov, V. A. G. K. *Rus. Chem. Bull.* **1997**, *46*, 874–880.
 (51) This value was found at www.h2o2.com, a site maintained by U.S. Peroxide, 2006.

was quantified by UV–vis at 700 nm. An amount of 2 equiv of $\mathbf{1}_{\text{red}}$ are consumed by each equiv of H_2O_2 . Preliminary experiments demonstrated that the kinetics of the reaction between $\mathbf{1}_{\text{red}}$ and H_2O_2 even under Ar are complex (polymodal). This precluded the detailed study of this reaction needed to determine rate constants for electron transfer to H_2O_2 . Therefore, other experiments using H_2O_2 were designed to assess whether observed rates of electron transfer from $\mathbf{1}_{\text{red}}$ to O_2 were compromised by contributions from the reaction of $\mathbf{1}_{\text{red}}$ with H_2O_2 (the first isolable and quantifiable product of reaction between $\mathbf{1}_{\text{red}}$ and O_2). For this, solutions of $\mathbf{1}_{\text{red}}$ were mixed in a stopped-flow apparatus with solutions uniformly saturated with O_2 , but that also contained a wide range of H_2O_2 concentrations. The initial rate of consumption of $\mathbf{1}_{\text{red}}$ (quantified by UV–vis), was plotted versus $[\text{H}_2\text{O}_2]$. This rate only slightly increased with addition of $[\text{H}_2\text{O}_2]$: the contribution to observed rates of electron transfer from $\mathbf{1}_{\text{red}}$ to O_2 from oxidation of $\mathbf{1}_{\text{red}}$ by H_2O_2 was found to be kinetically insignificant. Contributions were less than ca. 2–3% (i.e., less than experimental error) even at concentrations of H_2O_2 comparable to $\mathbf{1}_{\text{red}}$, much larger than those present during the acquisition of initial-rate data.

Kinetics Measurements. Reactions of $\mathbf{1}_{\text{red}}$ were carried out in water and in D_2O at pH(D) values of from 7.2 to 2, while reactions of $\mathbf{2}_{\text{red}}$ and $\mathbf{3}_{\text{red}}$ were carried out at pH 2. Unless indicated, ionic strength, μ , was kept constant at 175 mM. For reactions of $\mathbf{1}_{\text{red}}$ with O_2 , a series of solutions were used. Each solution contained NaCl along with 50 mM concentrations of the following buffer anions: pH 7.2 and 6.2 (phosphate), pH 4.5 (acetate), pH 3.0 (chloroacetate), and pH 2.0 (sulfate). To suppress Cu-catalyzed electron transfer to O_2 , diethylenetriaminepentaacetic acid (DTPA, pH 3 to 7) or 1,10-dimethylphenanthroline (neocuproine, pH 2) were added, as described below. When needed, NaCl or $\mathbf{1}_{\text{ox}}$ (in one experiment) was added to the second syringe. Reported total ionic strength values included all Na^+ or H^+ counter cations from the POMs, electrolyte, and buffer. The following general method, described in detail for reactions of $\mathbf{1}_{\text{red}}$, was used for all three reactions ($\mathbf{1}_{\text{red}}$, $\mathbf{2}_{\text{red}}$, and $\mathbf{3}_{\text{red}}$): One syringe in a stopped-flow apparatus was filled with an O_2 -free solution of $\mathbf{1}_{\text{red}}$. These solutions were diluted, as needed, with deaerated buffer solution such that, upon mixing, initial $[\mathbf{1}_{\text{red}}]$ values were between 0.05 and 1.0 mM. The second syringe in the stopped-flow apparatus was filled with solutions containing the same buffer solution (at the same concentration) but saturated with pure O_2 , or prepared by use of ambient-pressure O_2/Ar mixtures. At the routinely used ionic strength of 175 mM, saturation with pure O_2 at ambient pressure gave electrolyte solutions 1.15 mM in O_2 , a value 8% smaller than the solubility of O_2 in pure water. The same 8% correction was applied to calculate the concentrations of O_2 in solutions prepared using O_2/Ar mixtures. Changes in absorption with time were observed at a single wavelength, usually at or near 700 nm, and chosen after careful examination of the UV–vis spectra of $1e^-$ -reduced and fully oxidized α -Keggin anions. Because of the low solubility of O_2 in water at ambient pressure, it was not possible, within the sensitivity of the UV–visible spectrometer in the stopped-flow apparatus, to decrease initial $[\mathbf{1}_{\text{red}}]$ values to less than 10% of initial $[\text{O}_2]$ values. Therefore, the reactions were pseudo-first-order with respect to $[\text{O}_2]$ only in their initial stages (10 to 15% conversion). Initial rates were derived from absorbance versus time data, acquired during these early stages of the reactions, using standard software (KISS 5.1 for Macintosh).

Rate Constants. Rate constants were obtained using an iterative (self-consistent) form of the method of initial-rates. This method, described here in detail for reaction of $\mathbf{1}_{\text{red}}$, was used for all three anions. At each pH value (several for $\mathbf{1}_{\text{red}}$, and at pH 2 for all three donor anions), initial rates, r_1 , were measured over a range of $[\mathbf{1}_{\text{red}}]$ values at a specific initial $[\text{O}_2]$, and linear plots of r_1 versus $[\mathbf{1}_{\text{red}}]$ were obtained. Rates, r_1 , were measured in duplicate or triplicate, as necessary, to ensure reproducibility and accuracy. Linear plots of r_1 versus $[\mathbf{1}_{\text{red}}]$ were then obtained at several O_2 concentrations. The slopes of these plots, each at a unique $[\text{O}_2]$, are the apparent rate constants, k_{app} , where $-d[\mathbf{1}_{\text{red}}]/$

$dt = k_{\text{app}}[\mathbf{1}_{\text{red}}]$. Finally, for each pH value studied, k_{app} values were plotted as a function of $[\text{O}_2]$. These plots were linear, and their slopes gave the rate constants, k , associated with the rate expression $-d[\mathbf{1}_{\text{red}}]/dt = k[\mathbf{1}_{\text{red}}][\text{O}_2]$. (This iterative approach is more reliable than carrying out independent sets of experiments in which $[\text{O}_2]$ is varied at constant $[\mathbf{1}_{\text{red}}]$, and vice versa, because linear plots of k_{app} versus $[\text{O}_2]$ are only obtained if the data are internally self-consistent.) At the smallest and largest pH values studied, rate constants, k , were obtained for reactions carried out in D_2O . Standard experimental uncertainties were calculated using the “Regression” program from the “Data Analysis ToolPak” in MS Excel.

Note on Catalysis by Trace Quantities of Cu. Cu-ion catalysis of electron transfer to O_2 is well-known⁵² and was detected in the present work as well. In previous reports, we,⁵³ and others,⁵⁴ have noted that Cu ions are nearly always present as trace contaminants in aqueous electrolyte solutions.⁵⁵ In the present study, catalysis by traces of Cu was effectively eliminated by the addition of chelating agents. These were chosen for maximum effectiveness at the pH values at which the reactions were carried out. At pH values between 3.0 and 7.4, DTPA (20 to 40 μM) was added; at pH 2.0, neocuproine (40 μM) was used. These chelating agents limited Cu-ion catalysis to contributions of less than 2% of measured rate-constant values. Control experiments were carried out to ensure that neither DTPA nor neocuproine themselves (present at from 5 to 80 μM , and from 30 to 60 μM , respectively) had discernible effects on reaction rates.

Results

Reactions of the one-electron-reduced Keggin anions, $\alpha\text{-X}^{n+}\text{W}_{12}\text{O}_{40}^{(9-n)-}$, $\text{X}^{n+} = \text{Al}^{3+}$, Si^{4+} , P^{5+} , with O_2 were investigated using standard kinetic methods. All three anions were studied under conditions at which they are known (or were confirmed here) to be stable and effectively free of association with Na^+ or H^+ .⁵⁶ Reactions of $\mathbf{1}$, which is less well studied than $\mathbf{2}$ or $\mathbf{3}$, and is the only of these that is stable between pH 2 and 7.5, were investigated in the greatest detail and over a wide range of pH values. Kinetic data and rate constants for all three anions were then obtained at pH 2. In instances where specific information regarding $\mathbf{2}$ and $\mathbf{3}$ was not available from published reports, additional studies were carried out to confirm that all three anions $\mathbf{1}_{\text{red}}$, $\mathbf{2}_{\text{red}}$, and $\mathbf{3}_{\text{red}}$ behaved similarly. Analysis of the kinetic data, including use of the Marcus cross relation to estimate rates of electron transfer from POM_{red} to O_2 , and the effects of H^+ and POM charge, is left for the Discussion section.

Reaction Stoichiometry. A slight excess of O_2 was combined with $\mathbf{1}_{\text{red}}$ at pH 7.2 ($\text{NaH}_2\text{PO}_4/\text{Na}_2\text{HPO}_4$ buffer), and at pH 2 ($\text{NaHSO}_4/\text{Na}_2\text{SO}_4$ buffer), at 25 °C and a total ionic strength of $\mu = 175$ mM. Once the blue color associated with $\mathbf{1}_{\text{red}}$ had been discharged, H_2O_2 was identified and quantified by reaction with $\text{H}_5\text{TiPW}_{11}\text{O}_{40}$ ^{49,50} in 0.8 M H_2SO_4 , followed by UV–vis spectroscopic analysis of the resultant yellow peroxo-complex, $(\text{TiO}_2)\text{PW}_{11}\text{O}_{39}^{5-}$ (see Materials and Methods). At pH 7.2, a 0.44 mM solution of $\mathbf{1}_{\text{red}}$ gave a 0.23 mM solution of H_2O_2 (i.e., 0.52 equiv of H_2O_2 per equiv of $\mathbf{1}_{\text{red}}$ consumed). The same stoichiometry was observed at pH 2, at which a 0.50 mM solution of $\mathbf{1}_{\text{red}}$ gave a 0.26 mM solution of H_2O_2 (0.52 equiv

(52) Cher, M.; Davidson, N. *J. Am. Chem. Soc.* **1954**, *77*, 793–798.

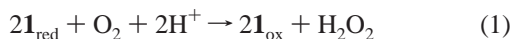
(53) Geletii, Y. V.; Bailey, A. J.; Boring, E.; Hill, C. L. *J. Chem. Soc., Chem. Commun.* **2001**, 1484–1485.

(54) Wang, X.; Stanbury, D. M. *J. Phys. Chem. A* **2004**, *108*, 7637–7638.

(55) Even after extensive efforts to obtain Cu-free solutions, Cu ions are still present at 1 to 2 μM concentrations (see ref 53).

(56) See refs 16 and 43 for recent aqueous-solution studies of $\mathbf{1}$ and for references to analogous data on $\mathbf{2}$ and $\mathbf{3}$.

of H₂O₂ per equiv of **1**_{red}). Therefore, at both pH 7.2 and 2, **1**_{red} reacts with O₂ according to eq 1. The same stoichiometry has been reported for reductions of O₂ by **2**_{red} and **3**_{red}.^{14,38}



Reactions of **1_{red}, **2**_{red}, and **3**_{red} with H₂O₂.** Additional control experiments showed that reduction of H₂O₂ by POM_{red} anions is sufficiently slow so as to make kinetically insignificant contributions to observed rate constants. For this, the effects of added H₂O₂ on observed initial rates of POM_{red} consumption by mixtures of O₂ (at a constant initial concentration) and H₂O₂ (over a range of initial concentrations) were determined (see Materials and Methods section). Initial reaction rates were plotted versus [H₂O₂] (see Supporting Information). In these plots, small increases in the rate of consumption of POM_{red} with increase in [H₂O₂] reflect small contributions from reaction of **1**_{red} with H₂O₂ to rates of reaction of **1**_{red} with O₂. For reactions of **1**_{red} and **2**_{red}, contributions from oxidation by H₂O₂ contribute less than 2–3% to observed rate constants for reduction of O₂. This value is smaller than the experimental errors, 3–5%, associated with measurements of rates of electron transfer to O₂ by these anions. For **3**_{red} at pH 1.3 (50 mM HCl), the relative rate of reduction of H₂O₂ is slightly larger than for **1**_{red} or **2**_{red}, but still small (<15%) over the entire range of concentrations at which initial-rate data for reactions with O₂ were recorded.

Order of Reaction with Respect to [POM_{red}]. A detailed description of the reaction between **1**_{red} and O₂ is provided here; data for reactions of **2**_{red} and **3**_{red} with O₂ are summarized at the end of the Results section. The order of reaction with respect to [**1**_{red}] was determined by measuring initial rates (*r*₁) as a function of initial **1**_{red} concentration, [**1**_{red}]₀ at constant initial [O₂] ([O₂]₀). The linear increase in initial rate, *r*₁ (–d[**1**_{red}]₀/dt) with increase in the [**1**_{red}]₀, over a wide range of [**1**_{red}]₀, showed the reaction to be first order with respect to [**1**_{red}]. The experiment was repeated at several [O₂]₀ values to confirm that the linear relationship between *r*₁ and [**1**_{red}]₀ was independent of [O₂]₀. For this, initial O₂ concentrations were varied by changing the partial pressures of pure O₂ in the O₂/Ar gas mixture used to saturate the buffer solutions combined at a 1:1 volume ratio with solutions of **1**_{red} in the stopped-flow instrument. The linear (first-order) dependence of (*r*₁) on [**1**_{red}]₀, at three [O₂]₀ values, corresponding to saturation of buffer solutions with 34, 56, and 100% O₂ (and to final concentrations, after mixing, of 0.20, 0.32, and 0.58 mM O₂), is shown in Figure 1.⁵⁷

Order of Reaction with Respect to [O₂]₀. The linear plots in Figure 1 are described by eq 2. The slopes of each of these lines are unique *k*_{app} values (in units of s^{–1}), associated with specific values of [O₂]₀.

$$-\text{d}[\mathbf{1}_{\text{red}}]_0/\text{d}t = k_{\text{app}}[\mathbf{1}_{\text{red}}]_0 \quad (2)$$

In an iterative, and hence highly accurate, form of the method of initial rates, *k*_{app} values were obtained for a series of [O₂]₀ values (as shown in Figure 1). The *k*_{app} values were then plotted as a function of [O₂]₀ (Figure 2).

(57) The non-zero—albeit small—value of the *Y*-intercept is due to small contributions to *r*₁ from the Cu-catalyzed pathway, which is not entirely eliminated even in the presence of DTPA.

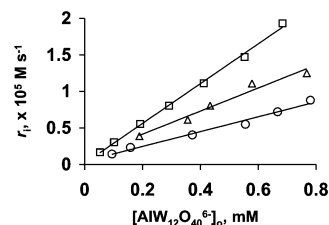


Figure 1. Dependence of initial rate *r*₁ (–d[**1**_{red}]₀/dt) on [AIW₁₂O₄₀^{6–}]₀ ([**1**_{red}]₀) at several initial concentrations of O₂ ([O₂]₀): 0.2 mM (○), 0.32 mM (△), and 0.58 mM (□) at pH = 7.2 and at 25 °C; 50 mM phosphate, 100 mM NaCl, and 25 μM DTPA (total ionic strength μ ≈ 175; value changes slightly during reaction).

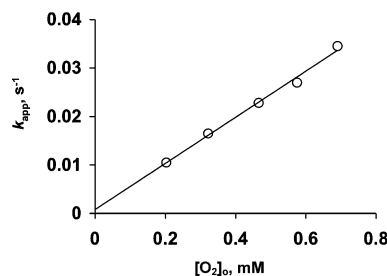


Figure 2. Dependence of apparent rate constants, *k*_{app}, on [O₂]₀ at pH = 7.2 and 25 °C: 50 mM phosphate, 100 mM NaCl, and 25 μM DTPA (total ionic strength μ ≈ 175).

The linear dependence (*R*² = 0.993) of *k*_{app} values on [O₂]₀ indicates the reaction is first order with respect to [O₂]₀ (eq 3). From the slope of the line in Figure 2, *k* = 48 ± 4 M^{–1}s^{–1}.

$$-\text{d}[\mathbf{1}_{\text{red}}]_0/\text{d}t = k[\mathbf{1}_{\text{red}}]_0[\text{O}_2]_0 \quad (3)$$

Additional Mechanistic Data. At constant [**1**_{red}]₀, observed rates, *r*₁ (–d[**1**_{red}]₀/dt), were determined as [NaCl] was increased from 10 to 810 mM (see Table S1 in Supporting Information). Over this range, the initial rates, *r*₁, decreased by ca. 25%. At the same time, initial concentrations of O₂, [O₂]₀, from saturation by pure O₂ (1 atm) decrease by ca. 25% over this range of ionic strength values.⁴⁸ The result is that rate constants, *k* (calculated using estimated [O₂]₀ values), remain effectively constant as [NaCl] is varied. This is consistent with a bimolecular reaction in which at least one of the reactants has a charge of zero. At the same time, more subtle effects, such as the effect of ionic strength on the free energy of formation of charged transition-state or successor complexes formed along the reaction coordinate could easily be “masked” by the uncertainty regarding the [O₂] present at each [NaCl]. Nonetheless, these data clearly rule out less subtle phenomena such as catalysis of the reaction by Na⁺. Significant ion pairing between **1**_{red} and Na⁺ is also ruled out: If present to an appreciable extent, reaction rates would decrease substantially¹⁴ with increase in [NaCl]. The absence of appreciable ion pairing is consistent with data for self-exchange between **1**_{red} and **1**_{ox}, in which reaction rates obey the extended Debye–Hückel equation over a similar range of [NaCl] and μ values.^{16,43}

At constant [**1**_{red}]₀, [O₂]₀, and ionic strength (μ), the addition of α-Na₅AIW₁₂O₄₀ (**1**_{ox}; from 0 to 10 mM, more than an order-of-magnitude larger than [**1**_{red}]₀) had no effect on *r*₁ (see Supporting Information). Addition of the defect “lacunary” ion, α-Na₉AIW₁₁O₃₉ (0 to 1 mM), or of Na₂WO₄ (0 to 0.2 mM) also had no effect on *r*₁. This rules out catalysis by tungstates that might be present—albeit at trace concentrations—in aqueous solutions of **1**_{red}.

Order of Reaction with Respect to $[H^+]$. The $[H^+]$ dependence of the reaction between \mathbf{I}_{red} and O_2 was evaluated by determining k (as defined in eq 3), at pH values of from 7.2 to 2. Ionic strength, μ , was kept constant at 175 mM; acid and Na^+ -salt forms of the following buffer anions (each at 50 mM) were used: phosphate (pH 7.2 and 6.2), acetate (pH 4.5), chloroacetate (pH 3.0), and sulfate (pH 2.0). At each pH value, the same procedure as that described in conjunction with Figure 1 was used: Rates, r_i , were obtained in duplicate or triplicate, at five to seven concentrations of \mathbf{I}_{red} . The slopes of plots of r_i versus $[\mathbf{I}_{\text{red}}]$ gave apparent rate constants, k_{app} . These k_{app} values were obtained at 5 $[O_2]_0$ values at pH 7.2 (ca. 75 measurements) and at 3 $[O_2]_0$ values at pH 2 (ca. 45 measurements). The rate constants, k (eq 3), obtained from plots of k_{app} obtained at these pH values, versus $[O_2]_0$, were effectively identical to one another. Once this was noted, additional data were obtained at intermediate pH values to rule out a change in mechanism near pH 4.69, the pK_a of HO_2^* , at which disproportionation between $O_2^{\bullet-}$ and HO_2^* is most rapid. For this series of experiments, two O_2 concentrations were used at each pH value (ca. 90 independent measurements). The results are listed in Table 1.

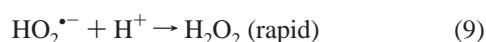
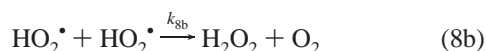
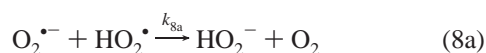
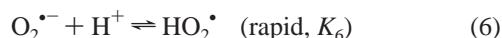
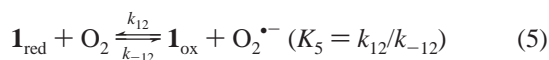
Solvent Kinetic Isotope Effects. Rate constants, k , were obtained for reactions in D_2O at the smallest and largest pH values studied (entries 2 and 7 in Table 1).

The data in Table 1 rule out a PCET mechanism by showing not only that the rate of oxidation of \mathbf{I}_{red} by O_2 is independent of pH, but also that the rate remains unchanged when the solvent, H_2O , is replaced by D_2O (i.e., no solvent kinetic-isotope effect is observed).⁵⁸

The above results are summarized in the following rate expression (eq 4).

$$-d[\mathbf{I}_{\text{red}}]/dt = k[\mathbf{I}_{\text{red}}][O_2][H^+]^0[\mathbf{I}_{\text{ox}}]^0 \quad (4)$$

Rate Constant, k_{12} , for Electron Transfer to O_2 . The relationship between the observed rate constant k in eq 4 and the rate constant, k_{12} , for the elementary step corresponding to electron transfer from \mathbf{I}_{red} to O_2 , is now defined. For this, it is necessary to discern which step(s) in the sequence of reactions (eqs 5–9) that ultimately give H_2O_2 is rate limiting.



Two plausible scenarios were considered: (1) Reactions in eqs 7 or 8 are rate limiting (a pre-equilibrium is rapidly established, with $K_5 = k_{12}/k_{-12}$, and relative reaction rates (r) are $r_{-12} \gg r_7$ or r_8) or (2) the reaction in eq 5 is rate limiting (and $r_{-12} \ll r_7$ or r_8). In both cases, the fate of $O_2^{\bullet-}$ and/or HO_2^* (from the equilibrium in eq 6) must be considered. Two rapid processes

Table 1. Rate Constants, k , for Reaction of $\alpha\text{-AlW}_{12}\text{O}_{40}^{6-}$ (\mathbf{I}_{red}) with O_2 at Several pH(pD) Values^a

entry	buffer	pH or pD	no. of $[O_2]$ evaluated ^c	k , $M^{-1} s^{-1}$
1	sulfate	2.0	3	48 ± 4^d
2	sulfate	2.0^b	2	47 ± 4
3	chloroacetate	3.0	2	48 ± 4
4	acetate	4.5	2	45 ± 4
5	phosphate	6.2	2	50 ± 4
6	phosphate	7.2	5	48 ± 4
7	phosphate	7.4^b	2	44 ± 4

^a Conditions: 25 °C, 50 mM buffer (conjugate–base anion), and total ionic strengths, μ , of 175 mM (from \mathbf{I}_{red} , buffer anions and counter cations, Na^+ and H^+ , and added $NaCl$). ^bpD in D_2O . ^c Number of O_2 concentrations at which linear plots of r_i versus $[\mathbf{I}_{\text{red}}]$, from duplicate or triplicate measurements of r_i , each at five to seven \mathbf{I}_{red} concentrations, were obtained. ^dUncertainties were calculated using the “Regression” program from the “Data Analysis ToolPak” in MS Excel.

involving these intermediates are plausible: HO_2^* could react with a second equiv of \mathbf{I}_{red} ($r_7 \gg r_8$) and/or the superoxide intermediates could disproportionate to give H_2O_2 and O_2 ($r_8 \gg r_7$). Reaction of \mathbf{I}_{red} with $O_2^{\bullet-}$ is absent because it is slow relative to the reaction of \mathbf{I}_{red} with HO_2^* . Not only is the reduction potential of HO_2^* substantially more positive (favorable) than that of $O_2^{\bullet-}$, the reaction between POM_{red} and $O_2^{\bullet-}$ is slow because of Coulombic repulsion between the anionic reactants.

If eq 7 is rate limiting, the rate expression would be $-d[\mathbf{I}_{\text{red}}]/dt = 2k_7K_5K_6[H^+][\mathbf{I}_{\text{red}}]^2[O_2][\mathbf{I}_{\text{ox}}]^{-1}$.⁵⁹ Here, the reaction is second order with respect to $[\mathbf{I}_{\text{red}}]$, inversely proportional to $[\mathbf{I}_{\text{ox}}]$, and pH dependent. This is ruled out by observation of a first-order dependence on $[\mathbf{I}_{\text{red}}]$, the absence of inhibition by $[\mathbf{I}_{\text{ox}}]$, and a zero-order dependence on $[H^+]$. If one of the reactions in eqs 8a or 8b is rate limiting, then $-d[\mathbf{I}_{\text{red}}]/dt = k_8K_5K_6[H^+]^n[\mathbf{I}_{\text{red}}]^2[O_2]^2$ ($n = 1$ or 2 , respectively, for eqs 8a or 8b). This, too, is in complete disagreement with the observed first-order dependence on both $[\mathbf{I}_{\text{red}}]$ and $[O_2]$. Thus, the forward reaction in eq 5, with rate constant k_{12} , is rate limiting.

The only remaining question is the relationship between k_{12} and the apparent rate constant, k , in eq 4: If $r_7 \gg r_{8a}$ or r_{8b} , then $k = 2k_{12}$. However, if r_{8a} or $r_{8b} \gg r_7$, then $k = k_{12}$. In both cases the overall reaction is independent of pH and its rate is controlled by k_{12} . To distinguish between these two possibilities, the ratios r_7/r_8 (rates of electron transfer from \mathbf{I}_{red} to HO_2^* , r_7 , relative to those of disproportionation, r_{8a} or r_{8b}) were evaluated at pH 7, 5, and 2. At pH 7 and 5, $r_{8a} > r_{8b}$, and the ratio r_7/r_{8a} (eq 10) was used; at pH 2 (well below 4.69, the pK_a of HO_2^*), r_7/r_{8b} (eq 11) was used.

$$\frac{r_7}{r_{8a}} = \frac{k_7[\mathbf{I}_{\text{red}}][HO_2^*]}{k_{8a}[HO_2^*][O_2^{\bullet-}]} = \frac{k_7[\mathbf{I}_{\text{red}}]}{k_{8a}[O_2^{\bullet-}]} \quad (10)$$

$$\frac{r_7}{r_{8b}} = \frac{k_7[\mathbf{I}_{\text{red}}][HO_2^*]}{k_{8b}[HO_2^*][HO_2^*]} = \frac{k_7[\mathbf{I}_{\text{red}}]}{k_{8b}[HO_2^*]} \quad (11)$$

Initial concentrations of \mathbf{I}_{red} were 1 mM, published values,⁶⁰

(58) In some cases involving tunneling, the kinetic isotopes effect (KIEs, k_H/k_D) may be small. Together, however, the absence of a solvent KIE and independence of observed rate constants on $[H^+]$ rule out a PCET mechanism. For more discussion of this see ref 34.

(59) For this, $K_6 = k_6/k_{-6} = [HO_2^*]/[H^+][O_2^{\bullet-}]$, $[HO_2^*] = K_6[H^+][O_2^{\bullet-}]$, and $[O_2^{\bullet-}] = K_{12}[\mathbf{I}_{\text{red}}][O_2]/[\mathbf{I}_{\text{ox}}] = \text{constant}$.

(60) Sawyer, D. T.; Valentine, J. S. *Acc. Chem. Res.* **1981**, *14*, 393–400.

respectively, for k_{8a} and k_{8b} , are 1×10^8 and $8.6 \times 10^5 \text{ M}^{-1} \text{ s}^{-1}$, and by conservative estimate (see full details in the Supporting Information) $k_7 \approx 10^8 \text{ M}^{-1} \text{ s}^{-1}$. Entry of these values into eqs 10 and 11 gives $r_7/r_{8a} = 1 \text{ mM}/[\text{O}_2^{\bullet-}]$ and $r_7/r_{8b} = 120 \times 1 \text{ mM}/[\text{HO}_2^{\bullet}]$. During the initial phase of the reaction between $\mathbf{1}_{\text{red}}$ and O₂, the steady-state concentrations of the rapidly consumed superoxide intermediates are several orders of magnitude smaller than $[\mathbf{1}_{\text{red}}]$. Hence, both ratios (eqs 10 and 11) are large.

Therefore, at all pH values studied, reduction of HO₂[•] by a second equivalent of $\mathbf{1}_{\text{red}}$ (eq 7) is sufficiently rapid that superoxide disproportionation (eqs 8a and 8b) is not kinetically significant. In addition, the estimated rate constant for electron transfer from $\mathbf{1}_{\text{red}}$ to HO₂[•] ($k_7 = 10^8 \text{ M}^{-1} \text{ s}^{-1}$) is many orders of magnitude larger than the observed rate constants, k , in Table 1 (ca. $48 \text{ M}^{-1} \text{ s}^{-1}$). These estimates, based on deliberately conservative assumptions, unambiguously identify electron transfer from $\mathbf{1}_{\text{red}}$ to O₂ as the rate-limiting step in the reduction of O₂ to H₂O₂ and show that the rate constant, k_{12} , for this step is defined as shown in eq 12 (i.e., $k = 2k_{12}$):

$$-d[\mathbf{1}_{\text{red}}]/dt = 2k_{12}[\mathbf{1}_{\text{red}}][\text{O}_2] \quad (12)$$

Electron Transfer from $\alpha\text{-X}^{n+}\text{W}_{12}\text{O}_{40}^{(9-n)-}$ ($\text{X}^{n+} = \text{Si}^{4+}$, P^{5+}) to O₂ at pH 2. At pH 2, and an ionic strength of 175 mM, kinetic measurements using $\mathbf{2}_{\text{red}}$ ($\text{X}^{n+} = \text{Si}^{4+}$) and $\mathbf{3}_{\text{red}}$ ($\text{X}^{n+} = \text{P}^{5+}$) gave $k(\text{Si}) = 17 \pm 2$ and $k(\text{P}) = 2.8 \pm 0.4 \text{ M}^{-1} \text{ s}^{-1}$ (k is the observed rate constant defined in eq 4). Significant contributions to observed rate constants from the oxidation of $\mathbf{2}_{\text{red}}$ or of $\mathbf{3}_{\text{red}}$ by the product, H₂O₂, were ruled out by control experiments involving mixtures of O₂ and H₂O₂ as described above for $\mathbf{1}_{\text{red}}$ (see Figure S1 in Supporting Information). In addition, electron transfer from $\mathbf{1}_{\text{red}}$ to O₂ is independent of $[\text{H}^+]$ at pH 2. The same was expected to hold true for reductions of O₂ by $\alpha\text{-Si}^{\text{IV}}\text{W}_{12}\text{O}_{40}^{5-}$ ($\mathbf{2}_{\text{red}}$) and $\alpha\text{-PW}_{12}\text{O}_{40}^{4-}$ ($\mathbf{3}_{\text{red}}$), whose charges are less negative than that of $\mathbf{1}_{\text{red}}$. This was confirmed for $\mathbf{2}_{\text{red}}$ and $\mathbf{3}_{\text{red}}$ by observing that no significant changes in rates occurred when the pH was decreased from 2 to 1. Finally, conservative calculations similar to those for $\mathbf{1}_{\text{red}}$ above (see Supporting Information) indicate that, at pH 2, rates of outersphere electron transfer from $\mathbf{2}_{\text{red}}$ or $\mathbf{3}_{\text{red}}$ to HO₂[•] are orders of magnitude larger than rates of superoxide disproportionation.⁶¹ These results are consistent with a common rate expression (eq 4) and mechanism (analogous to eqs 5–7) for electron transfer from all three Keggin anions to O₂ and indicate that the rate constants k_{12} for rate-limiting electron transfer from the reduced Keggin ions to O₂ are defined as shown in eq 12 (i.e., $k = 2k_{12}$). Therefore, for $\mathbf{2}_{\text{red}}$, $k_{12}(\text{Si}) = 8.5 \pm 1 \text{ M}^{-1} \text{ s}^{-1}$ and, for $\mathbf{3}_{\text{red}}$, $k_{12}(\text{P}) = 1.4 \pm 0.2 \text{ M}^{-1} \text{ s}^{-1}$.

(61) For $\mathbf{3}_{\text{red}}$ at pH 2, the estimated rate constant for electron transfer to HO₂[•] (k_{ET}) is $5 \times 10^7 \text{ M}^{-1} \text{ s}^{-1}$, so that the ratio in eq 11 becomes $r_{\text{electron transfer}}/r_{\text{disproportionation}} = 60 \times 1 \text{ mM}/[\text{HO}_2^{\bullet}]$. For $\mathbf{2}_{\text{red}}$, it was first necessary to estimate k_{11} for electron self-exchange at the prevalent ionic strength (see Discussion section for details). As described in the Supporting Information, the Marcus cross relation then gave $k_{\text{ET}} = 2 \times 10^8 \text{ M}^{-1} \text{ s}^{-1}$, so that the ratio in eq 11 ($r_{\text{electron transfer}}/r_{\text{disproportionation}}$) is equal to $240 \times 1 \text{ mM}/[\text{HO}_2^{\bullet}]$. The relatively small variation in calculated rate constants, k_{ET} , reflects variation in λ values of the Keggin anions, as well as in donor-anion charge, and the effect of the latter on corrected free energies used in the Marcus cross relation.

Discussion

Marcus Cross Relation. The Marcus cross relation (eqs 13–16)^{62–64} was used to estimate k_{12} values for reactions of all three anions, $\mathbf{1}_{\text{red}}$, $\mathbf{2}_{\text{red}}$, and $\mathbf{3}_{\text{red}}$, with O₂.

$$k_{12} = (k_{11}k_{22}K_{12}f_{12})^{1/2}W_{12} \quad (13)$$

$$\ln f_{12} = \frac{[\ln K_{12} + (w_{12} - w_{21})/RT]^2}{4 \ln(k_{11}k_{22}/Z^2) + (w_{11} + w_{22})/RT} \quad (14)$$

$$W_{12} = \exp[-(w_{12} + w_{21} - w_{11} - w_{22})/2RT] \quad (15)$$

The work terms, w_{ij} in $\ln f_{12}$ and W_{12} (eqs 14 and 15) are

$$w_{ij} = z_i z_j e^2 / D_s a [1 + \beta a (\mu)^{1/2}] \quad (16)$$

The constants, D_s and β , in eq 16 are the dielectric constant and reciprocal Debye radius, respectively, and values used were for water at 25 °C.^{16,43,65} The constant, e , corresponds to the charge of an electron, z_1 and z_2 are the charges of species present within binary precursor and successor complexes, a is the sum of the radii of reacting species, and μ is the prevalent ionic strength (175 mM). The work terms w_{ij} are too large to be ignored. However, one simplification is possible: because the charge on O₂ is zero, $w_{22} = w_{12} = 0$.

The rate constant, k_{22} , for electron self-exchange between O₂^{•-} and O₂ in water^{66,67} was determined directly using ¹⁶O₂^{•-} and ¹⁸O₂.⁶⁸ A k_{22} value of $450 \pm 160 \text{ M}^{-1} \text{ s}^{-1}$ was reported. However, in analysis of kinetic data for outersphere electron transfer from metallo-organic complexes to O₂, the Marcus cross relation gave “effective” rate constants for electron self-exchange between O₂^{•-} and O₂ (k_{22}) of between 1 and $10 \text{ M}^{-1} \text{ s}^{-1}$.⁶⁹ In reactions with a series of organic electron donors whose radii were between 5 and 7 Å (i.e., similar in size to the Keggin anion), the Marcus cross relation gave $k_{22} \approx 2 \text{ M}^{-1} \text{ s}^{-1}$.^{70,71} These “effective” k_{22} values are all ca. 2 orders of magnitude smaller than the directly determined value of $450 \pm 160 \text{ M}^{-1} \text{ s}^{-1}$. This discrepancy is attributed to the difference in size between the electron donors and O₂, whose “radius” is often approximated by the O–O bond length of 1.33 Å. Provided electron transfer occurs via an outersphere mechanism, these same trends should hold true for reactions of the Keggin anions ($r = 5.6 \text{ Å}$). This was assessed by using eqs 13–16 to estimate k_{12} values for reactions of all 3 anions with O₂.

Equilibrium Constants, K_{12} . Equilibrium constants, K_{12} (in eq 13), associated with the standard Gibbs free energies for electron transfer from the reduced Keggin anions to O₂ were calculated from electrochemical data. The reduction potentials, $E_{1/2}$, of all three Keggin-anion one-electron redox couples were

- (62) Marcus, R. A. *J. Phys. Chem.* **1963**, *67*, 853–857.
 (63) Marcus, R. A.; Sutin, N. *Biochim. Biophys. Acta* **1985**, *811*, 265–322.
 (64) Marcus, R. A. *Angew. Chem., Int. Ed.* **1993**, *32*, 1111–1121.
 (65) Kozik, M.; Baker, L. C. W. *J. Am. Chem. Soc.* **1990**, *112*, 7604–7611.
 (66) Ebersson, L.; Gonzalez-Luque, R.; Lorentzon, J.; Merchan, M.; Roos, B. O. *J. Am. Chem. Soc.* **1993**, *1154*, 2898–2902.
 (67) German, L.; Kuznetsov, A. M.; Efremenko, I.; Sheintuch, M. *J. Phys. Chem. A* **1999**, *103*, 10699–10707.
 (68) Lind, J.; Shen, X.; Merényi, G.; Jonsson, B. Ö. *J. Am. Chem. Soc.* **1989**, *111*, 7654–7655.
 (69) Zahir, K.; Espenson, J. H.; Bakac, A. *J. Am. Chem. Soc.* **1988**, *110*, 5059–5063.
 (70) Merényi, G.; Lind, J.; Shen, X.; Eriksen, T. E. *J. Phys. Chem.* **1990**, *94*, 748–752.
 (71) Merényi, G.; Lind, J.; Jonsson, M. *J. Am. Chem. Soc.* **1993**, *115*, 4945–4946.

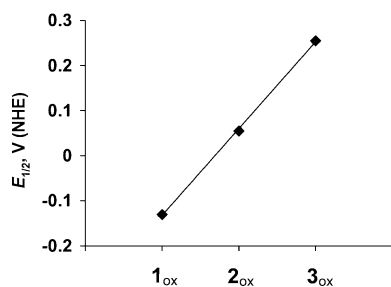


Figure 3. Linear ($R^2 = 0.9995$) variation in $E_{1/2}$ as a function of Keggin anion charge for one-electron reductions of 1_{ox} , 2_{ox} , and 3_{ox} , whose respective charges are 5-, 4-, and 3-.

Table 2. Kinetic and Energetic Parameters and Observed Rate Constants for Electron Transfer from One-Electron-Reduced Keggin Anions to O_2

Keggin anion	k_{11}^a $M^{-1} s^{-1}$	$E_{1/2}^c$ mV	ΔG° kcal mol $^{-1}$	K_{12}	k_{12}^e $M^{-1} s^{-1}$
1_{red} 1_{ox}	334 ± 75	-130	0.69	0.31	24 ± 2
2_{red} 2_{ox}	$(3.6 \pm 0.4) \times 10^5$ ^b	+55	5.2	1.5×10^{-4}	8.5 ± 1
3_{red} 3_{ox}	$(2.28 \pm 0.4) \times 10^7$	+255	9.6	9.0×10^{-8}	1.4 ± 0.2

^a Values for the **1** and **3** are experimental self-exchange rate constants measured at ionic strength $\mu = 175$ mM.^{16,65} ^b Estimated by setting λ_{in} for this self-exchange reaction equal to 12.2 kcal mol $^{-1}$, the mean of λ_{in} for **1** (15.5 kcal mol $^{-1}$) and for **3** (8.85 kcal mol $^{-1}$). By the use of Sutin's semiclassical method (refs 16 and 65), the λ_{in} value of 12.2 kcal mol $^{-1}$ gave a k_{11} value for $\mu = 0$ of 1.6×10^2 M $^{-1} s^{-1}$. The extended Debye-Hückel equation (ref 16) was then used to obtain k_{11} at $\mu = 175$ mM. The uncertainty represents an error of ± 1.7 kcal mol $^{-1}$ in estimation of λ_{in} (i.e., for $\lambda_{in} = 12.2 \pm 0.5[(15.5 - 8.85)/2]$ kcal mol $^{-1}$). ^c pH-independent values, obtained under conditions used for reactions with O_2 (pH 2 in NaCl and sulfate buffer; $\mu \approx 175$ mM). ^d From $\Delta G^\circ = -nFE^\circ$, where $E^\circ = E_{1/2}(O_2/O_2^{\bullet-}) - E_{1/2}(X^{n+}W_{12}O_{40}^{(8-n)-}/X^{n+}W_{12}O_{40}^{(9-n)-})$, at pH 2 in NaCl and sulfate buffer ($\mu \approx 175$ mM). ^e This work.

Table 3. Calculated and Observed Rate Constants, k_{12} , for Electron Transfer from α - $X^{n+}W_{12}O_{40}^{(9-n)-}$, $X^{n+} = Al^{3+}$, Si^{4+} , P^{5+} , to O_2 at pH 2

heteroatom X^{n+}	k_{12} $M^{-1} s^{-1}$	
	obsd	calcd
P^{5+}	1.4	12
Si^{4+}	8.5	3.8×10^2
Al^{3+}	24	7.9×10^2

determined under conditions identical to those used in reactions with O_2 . The data are consistent with the linear correlation between $E_{1/2}$ and Keggin-anion charge noted by Pope,⁴⁵ expanded here to include the $1_{ox}/1_{red}$ couple (Figure 3). Because rates of electron transfer are independent of $[H^+]$ between pH 2 and 7, the reduction potential of the $O_2(aq)/O_2^{\bullet-}(aq)$ couple was set equal to the pH-independent value of -0.16 V (NHE).⁷² The equilibrium constants, K_{12} , and additional constants, are collected in Table 2.

Calculation of k_{12} . To obtain $k_{12}(\text{calcd})$ values, the work term corrections, w_{11} and w_{21} , in f_{12} and W_{12} (eqs 14–15) were calculated using the constants in Table 2. The directly observed value of $k_{22} = 450$ M $^{-1} s^{-1}$ was used as the rate constant for self-exchange between O_2 and $O_2^{\bullet-}$, and radii of 5.6 and 1.33 Å, respectively, were assigned to the Keggin and superoxide anions. The results are listed in Table 3 (third column). As anticipated for outersphere electron transfer to O_2 , the calculated

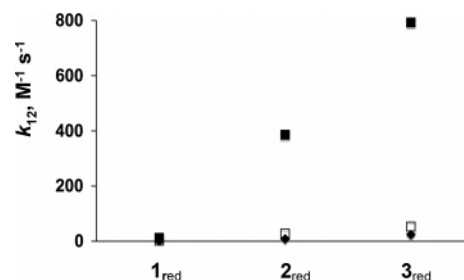


Figure 4. Observed (\blacklozenge) and calculated rate constants, k_{12} , for outersphere electron transfer from 1_{red} , 2_{red} , and 3_{red} to O_2 . Calculated rate constants were obtained from the Marcus cross relation (eq 13) using values of k_{22} of 450 M $^{-1} s^{-1}$ (\blacksquare) and 2 M $^{-1} s^{-1}$ (\square).

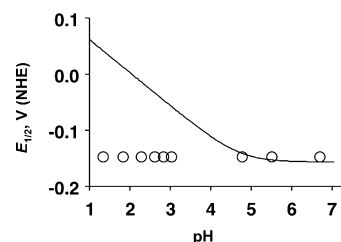
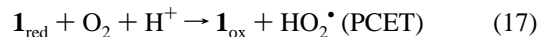


Figure 5. Reduction potentials of the $1_{ox}/1_{red}$ (circles) and $O_2(aq)/O_2^{\bullet-}$ (HO_2^{\bullet}) couples (solid line; calculated⁷⁴ using published values).⁷² As the pH drops below the pK_a of HO_2^{\bullet} (4.69), $E_{1/2}$ for the $O_2(aq)/O_2^{\bullet-}(HO_2^{\bullet})$ couple becomes more positive, and ΔG° for electron transfer to O_2 becomes more favorable.

rate constants, $k_{12}(\text{calcd})$, are each between ca. 1 and 1.5 orders of magnitude larger than the experimental values.^{70,71} However, when k_{22} is set equal to 2 M $^{-1} s^{-1}$, the results fall into reasonable agreement with observed values (rightmost column in Table 3 and Figure 4).⁷³

ET-PT versus PCET Mechanism. The reduction potential of the $O_2(aq)/O_2^{\bullet-}(HO_2^{\bullet})$ couple increases considerably as the pH drops below 4.69, the pK_a of protonated superoxide (HO_2^{\bullet}) (Figure 5).^{72,74} By contrast, 1_{red} is not protonated between pH values of 7 and 2; this is demonstrated by the invariance of $E_{1/2}$ with pH shown in Figure 5. As a result, 1_{red} is an ideal probe for evaluating the effect of $[H^+]$ (between pH 7 and 2) on rates of electron transfer from 1_{red} to O_2 : if H^+ is involved, its effect on the rate constant, k_{12} , for electron transfer to O_2 , is due exclusively to protonation of incipient $O_2^{\bullet-}$, but (*critically*) not to protonation of 1_{red} .

Two pathways are possible: (1) protonation of incipient $O_2^{\bullet-}$ by $H^+(aq)$ along the reaction coordinate of electron transfer from 1_{red} to O_2 (proton-coupled electron transfer, PCET; the single elementary step shown in eq 17) or sequential electron- and proton-transfer steps (an ET-PT mechanism; eqs 5 and 6, above).



One argument in favor of a PCET mechanism is that the implied

(73) The k_{22} values that, when used in the Marcus cross relation, bring calculated rate constants, $k_{12}(\text{calcd})$, fully into line with (*identical to*) observed k_{12} values are 3.1, 0.17, and 0.40 kcal mol $^{-1}$, respectively, for reactions of 1_{red} , 2_{red} , and 3_{red} . These specific k_{22} values are of questionable utility. This is because, while the small k_{22} value (2 M $^{-1} s^{-1}$) used in Figure 4 compensates for the difference in size (radii) between reacting species, this size difference is the same for all three Keggin-anion/ O_2 combinations. Therefore, k_{22} should, in principle, be the same for all three reactions. That this is not the case likely points to uncertainty in the effective radius of O_2 used to calculate the work terms, w_{ij} , in eq 16.

(74) MacInnes, D. A. *The Principles of Electrochemistry*, 1st ed.; Dover Publications, Inc.: New York, 1961.

(72) Chanon, M.; Julliard, M.; Santamaria, J.; Chanon, F. *New J. Chem.* **1992**, *16*, 171–201.

precursor complex, $[(\mathbf{1}_{\text{red}})(\text{O}_2)]^{6-}$ (i.e., $[(\text{AlW}_{12}\text{O}_{40})^{6-}(\text{O}_2)]^{6-}$), possesses a large negative charge. A reasonable question is whether this large negative charge might lead to hydrogen bonding between $\text{H}^+(\text{aq})$ and $[(\mathbf{1}_{\text{red}})(\text{O}_2)]^{6-}$, such that a vibrational mode of $\text{H}-\text{O}$ in protonated solvent, “ H_5O_2^+ ,” might be coupled with electron transfer from $\mathbf{1}_{\text{red}}$ to O_2 within the reacting species, $[(\text{AlW}_{12}\text{O}_{40})^{6-}(\text{O}_2)]^{6-}$. This would give $[(\text{AlW}_{12}\text{O}_{40})^{5-}(\text{HO}_2^\bullet)]^{5-}$ in a single PCET step. In most reported cases involving cationic metallo-organic complexes, such as $\text{Ru}(\text{NH}_3)_5\text{L}^{2+}$,^{69,75,76} outersphere electron transfer to O_2 is independent of $[\text{H}^+]$. Nonetheless, Stanbury and Taube argued that a PCET mechanism is most likely to occur when the electron donor (D), and hence, reacting pair (D:O₂), possess a smaller positive charge, as in $\text{Ru}(\text{NH}_3)_5\text{Cl}^{1+}$ (the charge is decreased from 2+ to 1+ by coordination of Cl^-), for which a first-order dependence on $[\text{H}^+]$ was observed.⁷⁶ By logical extension of this argument, PCET is even more likely to occur when the donor possesses a negative charge. Although less directly applicable, theoretical calculations⁷⁷ argue that outersphere electron transfer from a negatively charged Pt electrode to $\text{O}_2(\text{aq})$ (specifically when O_2 is not adsorbed on the electrode surface) occurs via a PCET mechanism.

The absence of a pH dependence or of a solvent kinetic isotope effect (Table 1) shows that, at pH values from 7 to 2, electron transfer from $\mathbf{1}_{\text{red}}$ to O_2 occurs via an outersphere ET–PT mechanism ($\mathbf{1}_{\text{red}}$ is the only anion of the series, $\alpha\text{-X}^{n+}\text{-W}_{12}\text{O}_{40}^{(9-n)-}$, $\text{X}^{n+} = \text{Al}^{3+}$, Si^{4+} , P^{5+} , that is stable over this pH range).

These findings do not, however, rule out the possibility of a PCET mechanism at lower pH values. Using Keggin anions that possess larger charges than those reported here, and/or at lower pH values, Darwent³⁰ observed a first-order dependence on $[\text{H}^+]$. This could involve either *intramolecular* proton transfer from the conjugate-acid form of a reduced cluster anion³⁴ or, as proposed by Darwent,³⁰ protonation of incipient superoxide radical anion by H^+ from solvent.³² Darwent’s proposal is intriguing from a practical perspective (catalyst design) but even more so from a fundamental one. It addresses the nature of protons and proton mobility in water, and ultimately, the validity of conventional notions regarding the innocence of the “solvent cage” within which aqueous electron-transfer processes occur.⁷⁸

Role of Donor-Anion Charge in Outersphere Electron Transfer to O₂. As X^{n+} in $\alpha\text{-X}^{n+}\text{W}_{12}\text{O}_{40}^{(9-n)-}$ is varied from P^{5+} to Si^{4+} to Al^{3+} (i.e., from $\mathbf{3}_{\text{red}}$ to $\mathbf{2}_{\text{red}}$ to $\mathbf{1}_{\text{red}}$), the driving force for electron donation to O_2 increases by nearly 0.4 V (a decrease in Gibbs free energy, ΔG° , of nearly 9 kcal mol⁻¹; Figure 3 and Table 2). Despite this, the associated increases in rates of electron transfer to O_2 are remarkably small (from 1.4 to 8.5 to 24 M⁻¹s⁻¹; Figure 4). This is due, in part, to a modest increase in the reorganization energies, λ , for self-exchange between reduced and oxidized forms of the Keggin anions, which vary from 25.2 to ca. 30 to 32.2 kcal mol⁻¹, respectively,¹⁶ for $\mathbf{3}$, $\mathbf{2}$, and $\mathbf{1}$ (see additional analysis in ref 81, below).⁷⁹ A second contributing factor is the effect of donor-anion charge. This is a direct consequence of the outersphere

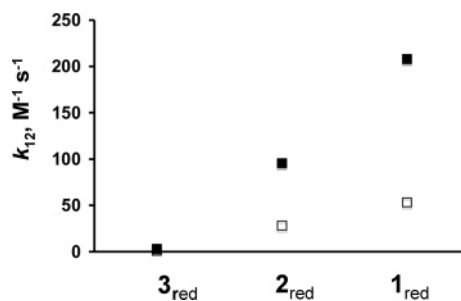


Figure 6. Inhibition of rate constants by electron-transfer-induced repulsion in the successor-complex ion pairs associated with each donor anion, i.e., $[(\mathbf{3}_{\text{ox}}^{3-})(\text{O}_2^{\bullet-})]^{4-}$, $[(\mathbf{2}_{\text{ox}}^{4-})(\text{O}_2^{\bullet-})]^{5-}$, and $[(\mathbf{1}_{\text{ox}}^{5-})(\text{O}_2^{\bullet-})]^{6-}$. The open squares (\square), 1.11, 23.8, and 53.3 M⁻¹ s⁻¹, respectively, are the values calculated using $k_{22} = 2 \text{ M}^{-1} \text{ s}^{-1}$ in Table 3 and Figure 4. The constants indicated by solid squares (\blacksquare) were obtained by simply setting the work terms, w_{21} , equal to zero in all three calculations.

ET–PT mechanism: As the Keggin anions become more negatively charged and better electron donors, the “successor-complex” ion pairs generated by electron transfer to O_2 are subject to larger anion–anion repulsions, which increase in the order $[(\mathbf{3}_{\text{ox}}^{3-})(\text{O}_2^{\bullet-})]^{4-} < [(\mathbf{2}_{\text{ox}}^{4-})(\text{O}_2^{\bullet-})]^{5-} < [(\mathbf{1}_{\text{ox}}^{5-})(\text{O}_2^{\bullet-})]^{6-}$. This attenuates the increase in rate that would otherwise accompany the larger driving forces associated with the more negatively charged donor anions. More precisely, electron transfer from the more negatively charged anions is associated with larger (and unfavorable) contributions to the kinetically relevant *corrected* Gibbs free energies, $\Delta G^{o'}$. (In the Marcus model, the corrected free energy, $\Delta G^{o'}$, is the difference in energy between the precursor and successor complexes, $[(\alpha\text{-X}^{n+}\text{W}_{12}\text{O}_{40}^{(9-n)-})(\text{O}_2)]^{(9-n)-}$ and $[(\alpha\text{-X}^{n+}\text{W}_{12}\text{O}_{40}^{(8-n)-})(\text{O}_2^{\bullet-})]^{(8-n)-}$, respectively. In eq 13, this is accounted for by rigorous inclusion of $\ln f$ and W).

The magnitude of the inhibition caused by anion–anion repulsion can be estimated by recognizing that corrections to ΔG° (to give $\Delta G^{o'}$) are equal to the Coulombic work terms, w_{21} (eq 16), associated with each electron-transfer reaction. At the prevalent ionic strength ($\mu = 175 \text{ mM}$), values of w_{21} are 0.94, 1.25, and 1.56 kcal mol⁻¹, respectively, for reactions of $\mathbf{3}_{\text{red}}$, $\mathbf{2}_{\text{red}}$, and $\mathbf{1}_{\text{red}}$. The increase in energy reflects the charge products, $z_1 z_2$, of the successor complexes, which increase from 3 to 4 to 5, respectively, for $[(\mathbf{3}_{\text{ox}}^{3-})(\text{O}_2^{\bullet-})]^{4-}$, $[(\mathbf{2}_{\text{ox}}^{4-})(\text{O}_2^{\bullet-})]^{5-}$, and $[(\mathbf{1}_{\text{ox}}^{5-})(\text{O}_2^{\bullet-})]^{6-}$. By setting w_{21} equal to zero, $\Delta G^{o'}$ reverts to ΔG° , the free energy that would be used to calculate K_{12} in eq 13 if no repulsion were present within the successor complexes.⁸⁰

The effect of setting w_{21} equal to zero for all three reactions is shown in Figure 6. The “leveling” of k_{12} that results from anion–anion repulsion (differences in rates between the solid and open squares) is significant. Moreover, the data in Figure 6 quantify the effects of electron-donor charge on the reduction of O_2 to $\text{O}_2^{\bullet-}$: when the oxidized (product) donor-anion possesses a charge of 3– (i.e., $\mathbf{3}_{\text{ox}}$), electron-transfer-induced

(75) Meyer, T. J.; Taube, H. *J. Chem. Phys.* **1968**, *7*, 2369–2379.

(76) Stanbury, D. M.; Haas, O.; Taube, H. *Inorg. Chem.* **1980**, *19*, 518–524.

(77) Anderson, A. B.; Albu, T. V. *J. Am. Chem. Soc.* **1999**, *121*, 11855–11863.

(78) Studies designed to better understand this are in progress. A key prerequisite (and challenge) is to fully define and control the protonation states of highly charged cluster anions at low pH values in water.

(79) While the $\text{W}_{12}\text{O}_{36}$ shells of $\mathbf{1}$, $\mathbf{2}$, and $\mathbf{3}$, are isostructural, $\text{X}^{n+}\text{-}\mu_4\text{-O}$ and $\mu_4\text{-O-W}$ bond distances vary slightly with heteroatom size and electronegativity. This accounts for the variation in λ values. See Sundaram, K. M.; Neiwert, W. A.; Hill, C. L.; Weinstock, I. A. *Inorg. Chem.* **2006**, *45*, 958–960.

(80) When setting $w_{21} = 0$, uncertainty associated with the calculation of actual (non-zero) w_{21} values—the result of the nonspherical shape of O_2 and its small size relative to that of the Keggin anions—is of no concern. When calculated using the “uncorrected” ΔG° values for the reduction of O_2 to $\text{O}_2^{\bullet-}(\text{aq})$ by $\mathbf{3}_{\text{red}}$, $\mathbf{2}_{\text{red}}$, and $\mathbf{1}_{\text{red}}$, rate constants for $w_{21} = 0$ in Figure 6 are, respectively, 3, 96, and 208 M⁻¹ s⁻¹.

anion–anion repulsion results in an approximately 3-fold decrease in rate; for \mathbf{I}_{ox} (a 5^- ion) an approximately 4-fold decrease is predicted. This analysis also provides an additional—albeit indirect—line of evidence that the reactions are both outersphere in nature and occur by an ET-PT, rather than a PCET, mechanism.⁸¹

One general implication is that efforts to increase rates of outersphere electron transfer¹⁴ to O_2 in catalysis,^{5,9} photocatalysis,¹³ or in electro-catalytic processes^{8,10–12} by using heteropolytungstates that possess more negative charges (associated with more negative reduction potentials) may face inherent limitations imposed by increased repulsion in successor–complex ion pairs.

Conclusions

The data in Figures 4 and 6 demonstrate that electron transfer from reduced Keggin heteropolytungstates to O_2 occurs via outersphere electron transfer. As a result, the outstanding ambiguity regarding the inner vs outersphere nature of this general and representative reaction is now resolved.⁸² This conclusion is consistent with product-analysis studies of polytungstates with O_2 , where natural-abundance ^{17}O NMR showed that “ O^{2-} anions” were first present in H_2O before being observed through ligand exchange in the POM structure.³⁹ These findings are readily understood when one considers that (1) the

six large O^{2-} ligands coordinated to each W atom⁸³ inhibit access of O_2 to W and (2) the six W–O bonds within each WO_6 unit are relatively inert.

The “leveling” of k_{12} that results from anion–anion repulsion (Figure 6) provides an additional line of evidence that the reactions are both outersphere in nature and occur by an ET–PT, rather than by a PCET, mechanism. This is directly applicable to reactions with O_2 under turnover conditions in catalysis. Namely, efforts to increase rates of electron transfer to O_2 through the use of heteropolytungstate cluster anions that possess more negative charges and reduction potentials face an inherent limitation imposed by corresponding increases in anion–anion repulsion within successor–complex intermediates.

More generally, the data in Figure 6 show the extent to which electron-donor charge influences actual rates of outersphere electron transfer to O_2 . Although this phenomenon is addressed in familiar models, such as that of Marcus, the data in Figure 6 are useful because they provide a quantitative estimate of its true influence. Moreover, just as negatively charged donors inhibit the reaction rate, positively charged donors should increase it (and to a similar extent). Therefore, these findings are applicable to outersphere processes in which any neutral molecule is converted to an anion via an ET or ET–PT mechanism.

Acknowledgment. We thank the DOE (DE-FC36-95GO10090), the U.S. Department of Agriculture (Grant FS-FPL-4709), TEKES (National Technology Agency of Finland), and PSC CUNY (Grant 60088-35-36) for support.

Supporting Information Available: Reactions of $\mathbf{1}_{\text{red}}$, $\mathbf{2}_{\text{red}}$, and $\mathbf{3}_{\text{red}}$ with O_2 in the presence of H_2O_2 (Figure S1); the effect of NaCl on the rate of reaction of $\mathbf{1}_{\text{red}}$ with O_2 (Table S1); the effect of $\alpha\text{-AlW}_{12}\text{O}_{40}^{5-}$ ($\mathbf{1}_{\text{ox}}$) on the rate of reaction of $\mathbf{1}_{\text{red}}$ with O_2 ; estimation of the rate constant, k_7 for the reaction in eq 7 of the text. This material is available free of charge via the Internet at <http://pubs.acs.org>.

JA064244G

(81) As noted above, the increase in λ values also contributes to the leveling of k_{12} values. For example, estimates indicate that if λ for a self-exchange between reduced and oxidized forms of $\mathbf{3}$ (i.e., $25.2 \text{ kcal mol}^{-1}$), the observed rate constant, k_{12} , for reaction of $\mathbf{1}_{\text{red}}$ with O_2 would increase by an amount similar to that obtained by setting $w_{21} = 0$ in Figure 6. However, the effect of variation in charge is much more significant: (1) it provides support for the ET–PT mechanism, (2) it is generally applicable to all outersphere reactions of charged donors with O_2 , and (3) it is rarely observed, let alone quantified. In this regard, it bears noting that all values in Figure 6 are calculated using *experimental* k_{11} values, and therefore, the results are *entirely independent of the underlying variation in λ values*.

(82) The dependence of rate constants on $[\text{H}^+]$ in ref 38, which led to the proposal of an innersphere pathway, may have been due to the large changes in alkali-metal cation concentration associated with large variation in pH at constant ionic-strength values of 0.5 M (i.e., $[\text{Na}^+]$ values varied by nearly 0.5 M). That work is reviewed in ref 14.

(83) Radii are typically ca. 1.2 \AA for 2-coordinate O^{2-} anion and 0.74 \AA for 6-coordinate W(VI): from Huheey, J. E. *Inorganic Chemistry: Principles of Structure and Reactivity*, 2nd ed.; Harper and Row: New York, 1978.